Research Article

Global warming and groundwater from semi-arid areas: Essaouira region (Morocco) as an example

Bahir Mohammed[1,2] · Ouhamdouch Salah[2] · Ouazar Driss[1] · Chehbouni Abdelghani[1,3]

Received: 12 March 2020 / Accepted: 8 June 2020 / Published online: 18 June 2020

Abstract
Climate change is undoubtedly becoming a subject of great concern for public authorities in all regions of the globe, in particular, the regions under Saharan, arid, and semi-arid climate. In this regard, this study aims to assess the effect of climate change on groundwater from semi-arid environments, taking the Essaouira basin as an example. The climate approach shows a downward trend in precipitation from 12 to 16% and an increase in temperature from 1.2 to 2.3 °C, and this during the last three decades. A continuous decline in the piezometric level exceeding 12 m for the Cenomanian–Turonian aquifer and 17 m for the Plio-Quaternary aquifer has been observed. The groundwater mineralization is controlled by the dissolution of evaporate and carbonate minerals, by the bases exchange phenomenon, and by the marine intrusion, especially in Plio-Quaternary aquifer. Also, the groundwater quality in the study area deteriorates gradually over time and space. However, the results of this study confirm that the groundwater from Essaouira basin is vulnerable to the global warming.

Keywords Semi-arid area · Climate change · Groundwater · Piezometry · Hydrochemistry

1 Introduction

Global warming is a global phenomenon. This phenomenon generates long-term complex interactions between environmental factors and economic and social conditions leading to remarkable effects at the regional scale [1, 25], especially at the Mediterranean level [5, 14, 28].

In areas under a Saharan, arid, and semi-arid climate, the precipitation is the determining factor for climatic characterization. The study of their recent evolution and climate variability is emerging essential for finding solutions to the problems of water availability [5–7, 9, 33].

In the Maghreb countries, studies on climate change show that the global warming is more significant than the average observed on a global scale. In fact, on a global scale, the warming is estimated at 0.74 °C during the twentieth century, while it fluctuates between 1 and 2 °C on the Mediterranean and North African scales [17, 19, 28, 33]. As for precipitation, it decreases in the Mediterranean region, in the Sahel, in southern Africa, and in certain parts of South Asia at different temporal and spatial scales [1, 18].

Morocco, one of the countries under arid and semi-arid climate, remains one of the most vulnerable to the climate change effects. It is characterized by a spatio-temporal irregularity in precipitation, becoming weaker towards the south [35]. This country has suffered from several periods of drought [3, 4, 12]. Several studies of precipitation within Morocco have shown that the number of dry periods is greater than the number of wets periods, with a general downward trend of 23% [5, 12, 28, 30, 36]. As for the temperatures, they show an increasing trend with warming varying between 0.3 and 2.5 °C depending on the region [3, 28, 30].

✉ Bahir Mohammed, bahir@uca.ac.ma | [1]IWRI, Mohammed VI Polytechnic University, Hay My Rachid, 43150 Ben Guerir, Morocco. [2]High Energy and Astrophysics Laboratory, Faculty of Sciences Semlalia, Cadi Ayyad University, P.O.B. 2390, 40000 Marrakesh, Morocco. [3]Centre d'Etudes Spatiales de la Biosphère, Université de Toulouse, CNES, CNRS, IRD, UPS, 31400 Toulouse, France.

However, this change in climate parameters caused by climate change is likely to have a negative effect on water resources, especially in areas under Saharan, arid, and semi-arid climate.

The Essaouira basin (Western Morocco) characterized by a semi-arid climate [27] is probably no exception to these effects. However, this investigation aims to evaluate the climate change impact on water resource within the basin by combining the climatic, piezometric, and hydrochemical techniques.

2 Study area

The Essaouira basin, the objective of this study, is part of the Atlantic Atlas, which is the westernmost part of the southwestern Moroccan basin [11, 13]. This basin is bounded to the north by Hadid anticline, to the south by Igrounzar and Tidzi wadis, to the east by the Bouabout region, and to the west by the Atlantic Ocean. It is subdivided into two parts, the first known as the "Bouabout unit" (upstream part) and the second known as the "coastal zone" (downstream part) (Fig. 1).

From a morphological point of view, the study area is made up of a set of synclinal basins filled with formations ranging from the Triassic to the Quaternary with elevations varying between 0 and 1600 m. Hydrographically, it is characterized by a less-developed network and this is represented by Ouazzi wadi in the north and Igrounzar wadi in the south for the upstream part and by Ksob and Tidzi wadi for the downstream part (Fig. 2).

Geologically and hydrogeologically, the upstream part is marked by the outcrop of formations of Middle and Upper Cretaceous age, in particular, Albian-Vraconian, Cenomanian, and Turonian [2, 13] (Fig. 2). These formations are composed of limestone and dolomitic benches interspersed with marl and sandstone. The Albian-Vraconian formations contain sandstone and limestone dolomites alternating with sandstone banks and sandy clays.

The Cenomanian (about 200 m thickness) is represented by alternating marls with anhydrite, lumachellic, and dolomitic limestones. As for the Turonian, it is composed of

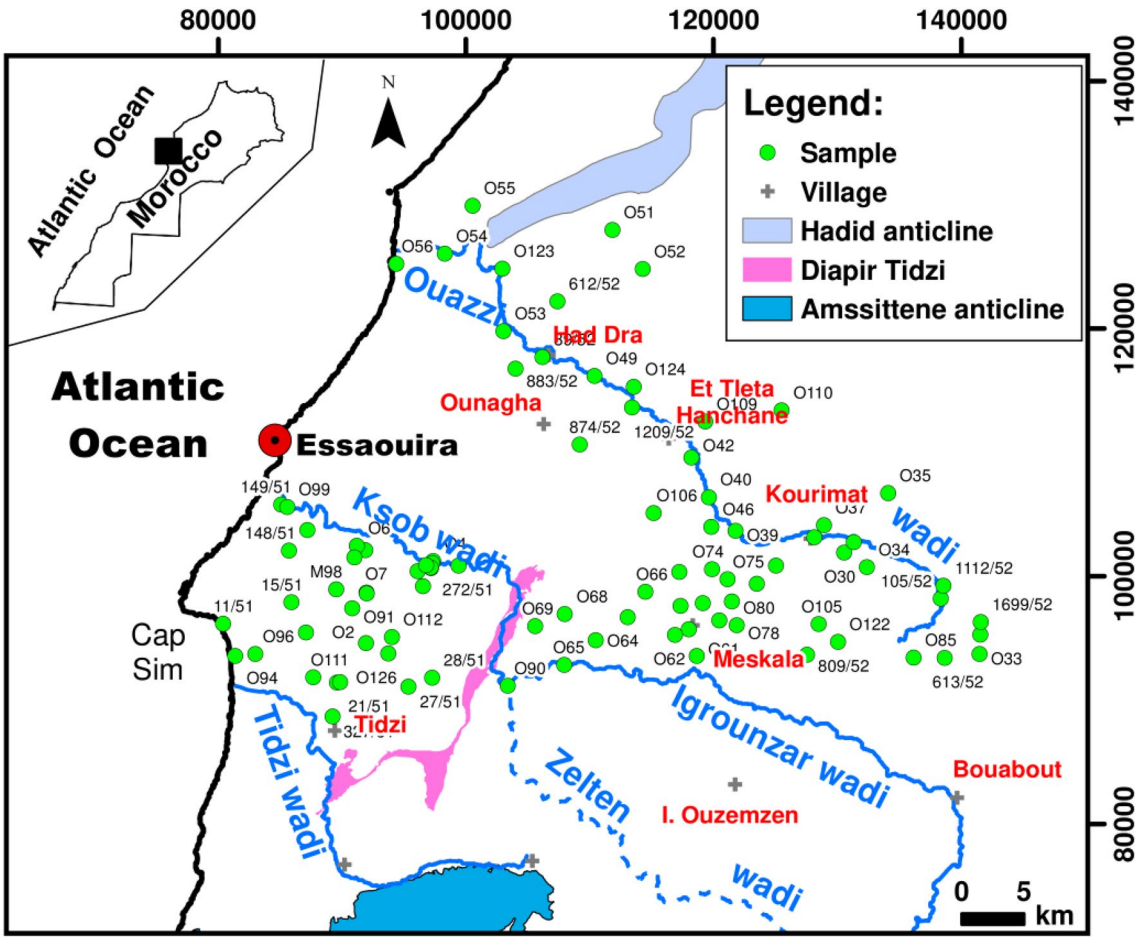

Fig. 1 Location of study area

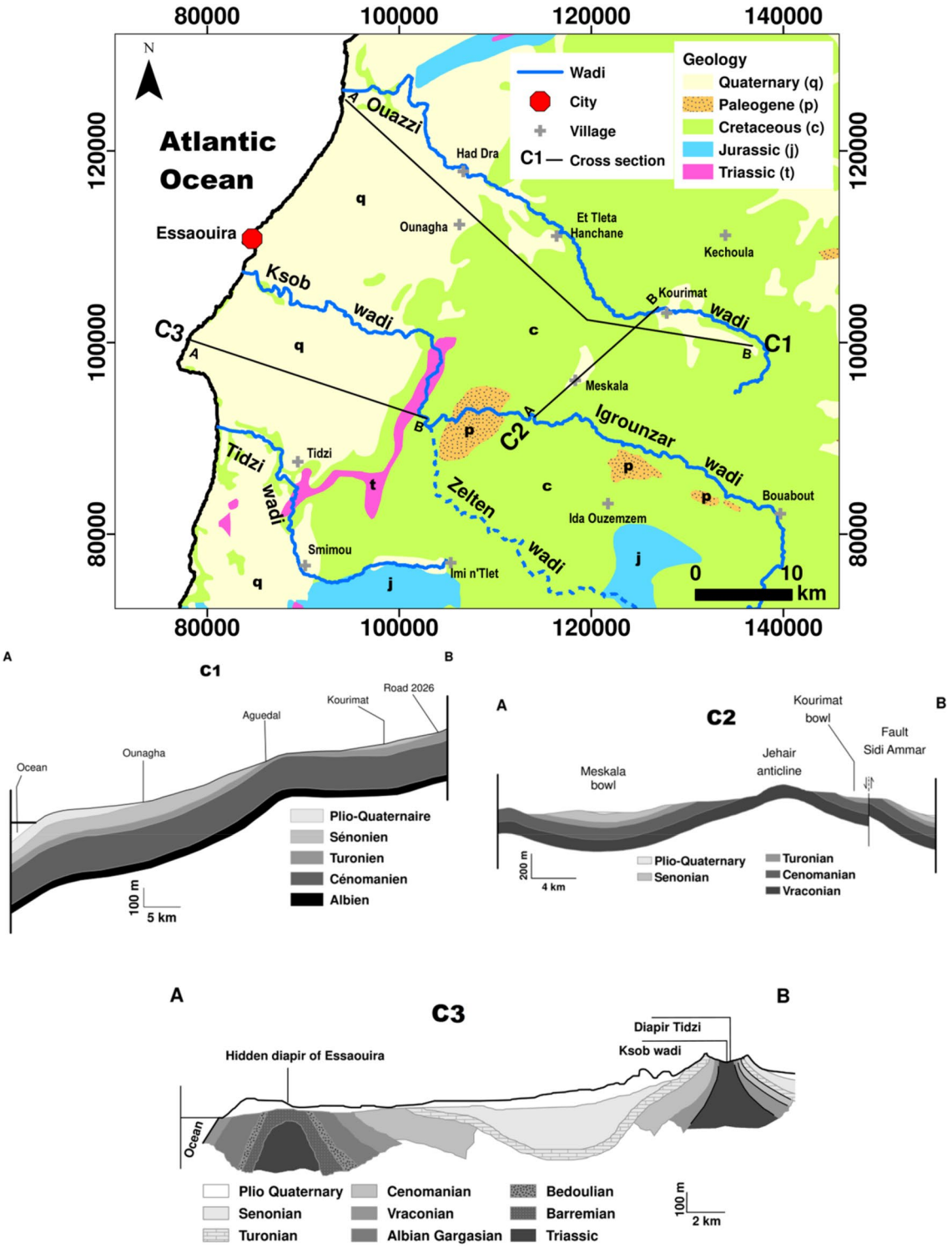

Fig. 2 Geological map of study area and cross section location

limestones with an abundance of silica. These synclines contain important water reservoirs (aquifer), notably the Cenomanian–Turonian aquifer which remains the most important in the region. According to Jalal et al. [20], this aquifer has transmissivities varying between $2.2*10^{-4}$ and $2.7*10^{-1}$ m^2/s.

The downstream part contains two important aquifers: (1) the Plio-quaternary and (2) the Turonian (Fig. 2).

The Plio-quaternary is characterized by a matrix of limestone sandstone. It contains an important water table, the wall of which is formed in the synclinal structure by the marls of Senonian (Fig. 2).

According to Mennani [24], this water table has transmissivities varying between $6.1*10^{-2}$ and $4.5*10^{-5}$ m^2/s.

As for the Turonian, represented by limestones, it contains a captive aquifer under the Senonian marls in the synclinal structure and probably in direct contact with the Plio-Quaternary at the confines of this structure (Fig. 2). It has a transmissivity ranging between $0.8*10^{-4}$ and $2.7*10^{-2}$ m^2/s [24].

3 Materials and methods

In this investigation, the results of nine campaigns 1990, 1995, 2007, 2009, 2015, 2016, 2017, 2018, and 2019 were used to assess the quality of groundwater in the Essaouira region in the context of climate change. Electrical conductivities, temperatures, pH, and nitrates were measured in situ, and the depth of the water level was measured using a 200 m piezometric probe.

The analyses of chemical elements were carried out at the Laboratory of Hydrogeology at the Faculty of Sciences Semlalia (Marrakech, Morocco) for the campaigns 1990–2009. As for that of 2015–2019, the analyses were carried out at the Laboratory of Geosciences and Environment—ENS at the Ecole Normale Superieure (Marrakech, Morocco). The SO_4 anion contents were determined by the nephelometric method [34]. Concentrations of Ca and Mg cations were measured by the complexometry method (EDTA) and those of Cl by the Mohr method [34]. The Na and K contents were determined by flame photometry [34]. As for HCO_3 contents, they were determined by titration using a sulphuric acid solution. All the samples display an ion balance of less than 10%, which allowed us to validate the obtained results. The obtained results are grouped in "Appendix".

4 Results and discussion

4.1 Climatic parameters

The climate parameter data used in this study were obtained from the Tensift Hydraulic Basin Agency (ABHT). On an annual scale, the analysis of precipitation data for an observation period of 38 years (1978–2015) for the study area reveals significant variability (Fig. 3).

Indeed, this rainfall is subject to fluctuations from 1 year to another, with wet and other dry periods of two to five consecutive years. Precipitation rates vary between a minimum of 135 mm, measured during the hydrological year 2007/08 and a maximum of 707 mm during the year 1995/96 with an average of 304 mm.

The application of the Pettitt test [31] (Table 1) with a 90% confidence level shows the presence of a break in the precipitation series in 1998/97. The average of annual rainfall before and after this break is 313.8 and 263.4 mm, respectively. This makes it possible to estimate a rainfall deficit of 16%. The results of the Mann–Kendall test (Table 1) display a negative multivariable standard normal (U_{MK}) ($U_{MK} = -1.09$). This reflects a downward trend in precipitation and confirms the results of the Pettitt test.

The evolution study of annual atmospheric temperatures was carried out over for 28 years (1987–2015). Maximum temperatures range between 29.3 and 37.2 °C with an average of 34.2 °C. As for the minimum temperatures, they range between 2.4 and 9.3 °C with an average of 7.4 °C, while the average temperatures vary between 17.7 and 22.4 °C with an average of 20 °C (Fig. 4a).

The application of the Pettitt test with a significance level equal to 5% shows the existence of a significant break in the series of maximum, average, and minimum annual temperatures, respectively, in 1999, 2000, and 1994 (Fig. 4b). For the maximum annual temperatures, the average before and after this break is 32.75 and 35.53 °C, with an increase of 2.8 °C. As for the mean annual temperatures, the average before and after the break is equal to 18.85 and 21.13 °C, respectively, with a warming of 2.3 °C. For minimum annual temperatures, the average before and after the break is 5.66 and 8.14 °C, respectively, with an increase of 2.5 °C.

This upward trend is corroborated by the Mann–Kendall test with a positive multivariable standard normal UMK for annual maximum temperatures ($U_{MK} = +5.24$), annual mean temperatures ($U_{MK} = +5.65$), and annual minimum temperatures ($U_{MK} = +4.65$).

4.2 Piezometry

The groundwater piezometric level evolution is closely related to the variation in precipitation [5, 26], the degree of exploitation and the contributions of surface water.

The piezometric maps drawn up from the data of 1990, 1995, 2007, 2015, 2016, 2017, 2018, and 2019 companions for the aquifers within the Essaouira basin show that:

- For the upstream part, the groundwater has a general flow direction from SE to NW for the southern part and from NE-SW for the northern part (Fig. 5a). This flow is conditioned by the substratum of the studied reservoir. Over a 24-year observation period (1995–2019), the groundwater maintains the same flow direction with a decline in the piezometric level. This decline is manifested, for

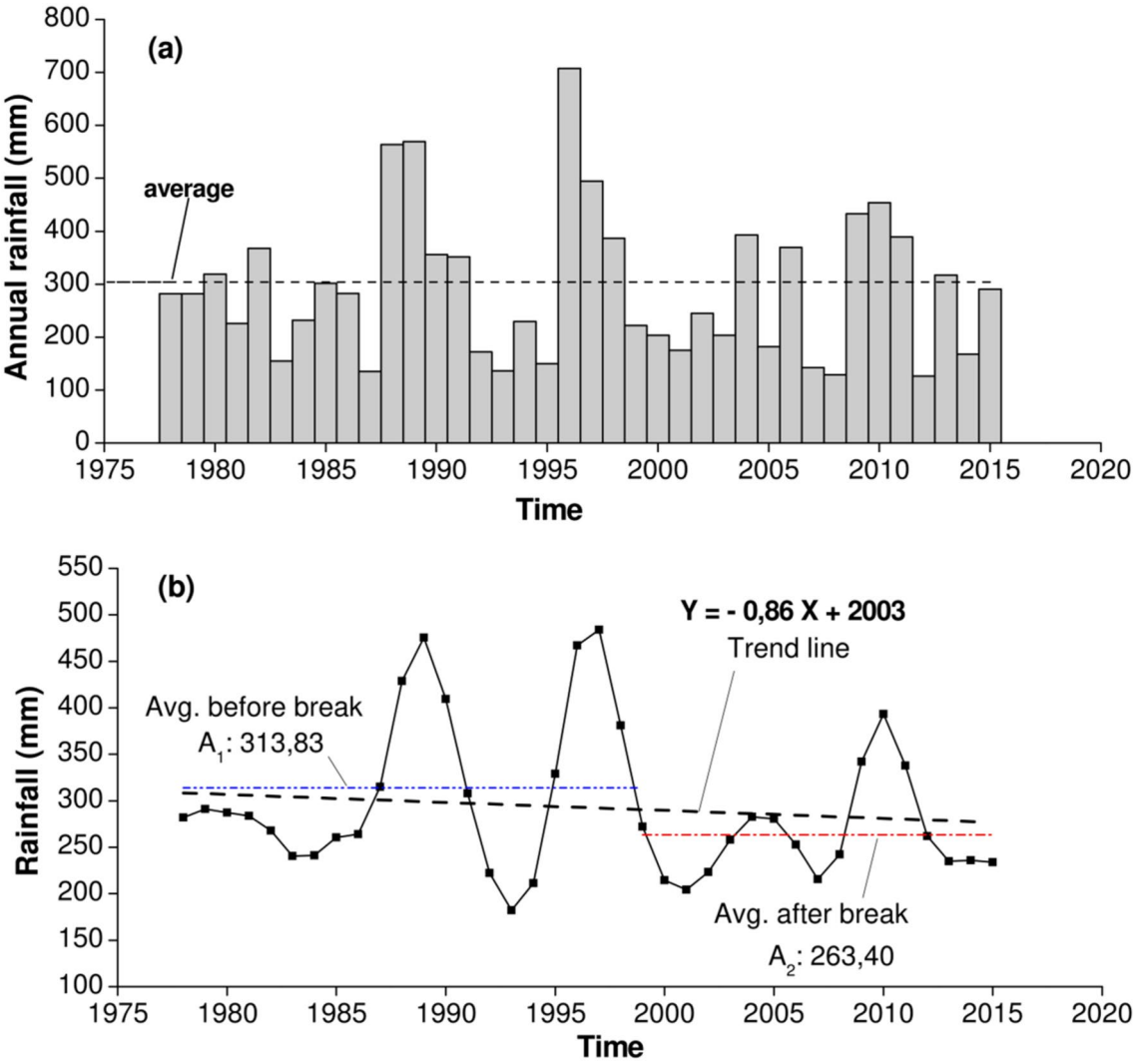

Fig. 3 **a** Annual precipitations and **b** Pettitt test results

Table 1 Statistical tests

Test	Formula	References
Pettitt	$U_{tT} = \sum_{i=1}^{t} \sum_{j=i+1}^{T} D_{ij}$	Pettitt [31]
	With: $D_{ij} = -1\ si\ (x_i - x_j) > 0,\ \ D_{ij} = 0\ si\ (x_i - x_j) = 0,\ \ D_{ij} = 1\ si\ (x_i - x_j) > 0$	
Mann–Kendall	$U_{MK} = \frac{S}{\sqrt{\mathrm{Var}(s)}}$	Mann [22] Kendall [21]
	With: $S = \sum_{i=1}^{n-1} \sum_{j=i+1}^{n} \mathrm{sgn}(a_j - a_i)$ and $\mathrm{Var}(s) = \frac{n(n-1)(2n+5)}{18}$	
	The trend is upward if $U_{MK} > 0$, downward if $U_{MK} < 0$	

example, by the offset of the piezometric curves 450 and 600 m more and more to the upstream, and this on the two piezometric maps (Fig. 5a).

The piezometric level evolution of the wells, capturing the Cenomanian–Turonian aquifer, whose water level measured in 2007, 2016, 2017, 2018, and 2019, is presented in Fig. 6. From this, all the wells show a decline in

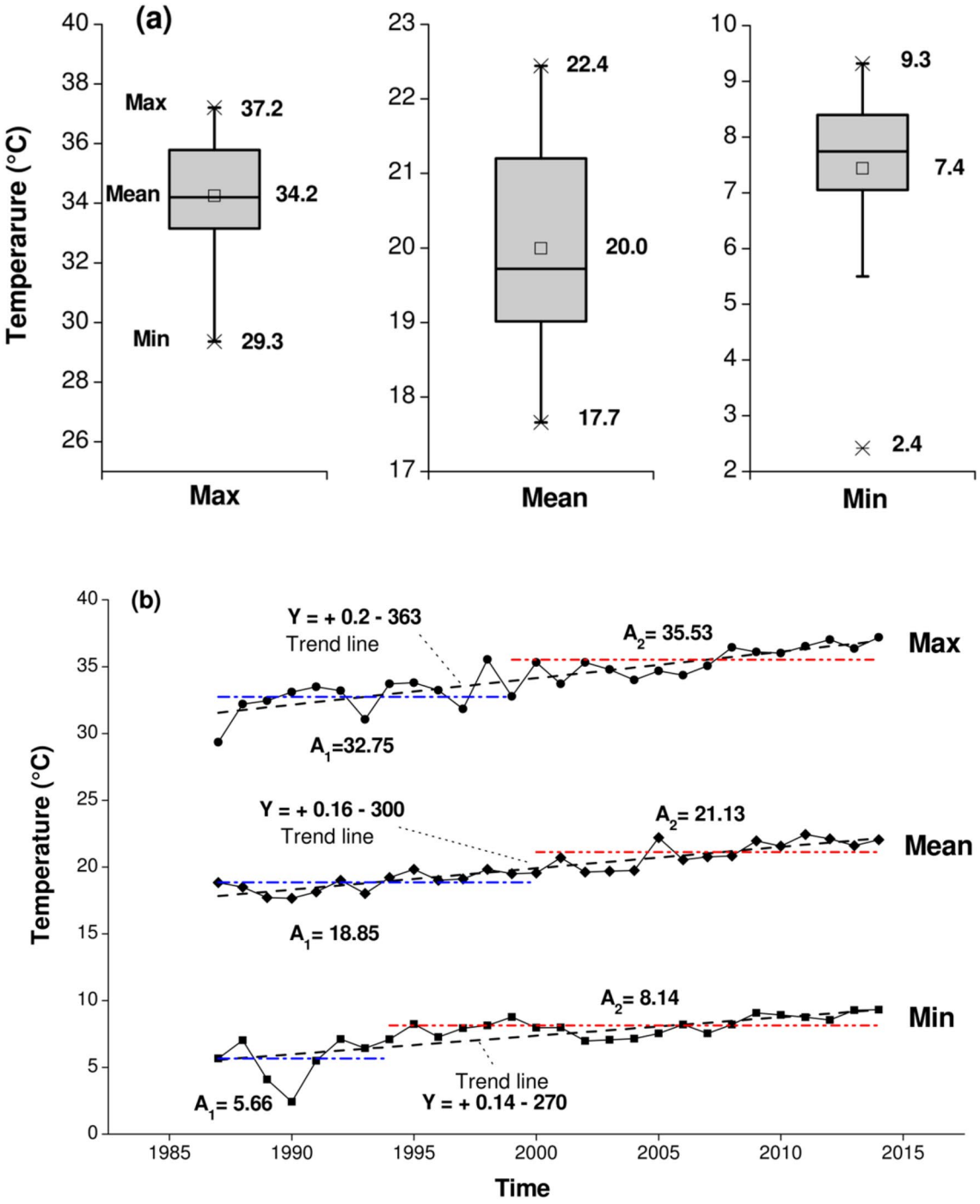

Fig. 4 **a** Maximum, average, and minimum temperatures, **b** Pettitt test results

their piezometric levels. It reached 9.3 m at well O30 and 12.6 m at well 75/52 between 2007 and 2019.

- For the downstream part, the general direction of groundwater flow of the Plio-Quaternary aquifer is generally from south-east to north-west (Fig. 5b). The groundwater flow within the Plio-Quaternary aquifer is imposed by the inclination of its substratum. The same remark was observed in the downstream part; the groundwater keeps the same direction of the flow with a decline in the piezometric level. Over a 29-year observation period (1990–2019) (Fig. 5b), the groundwater keeps the same flow direction with a decline piezometric level. This situation is materialized, for example, by the offset of the

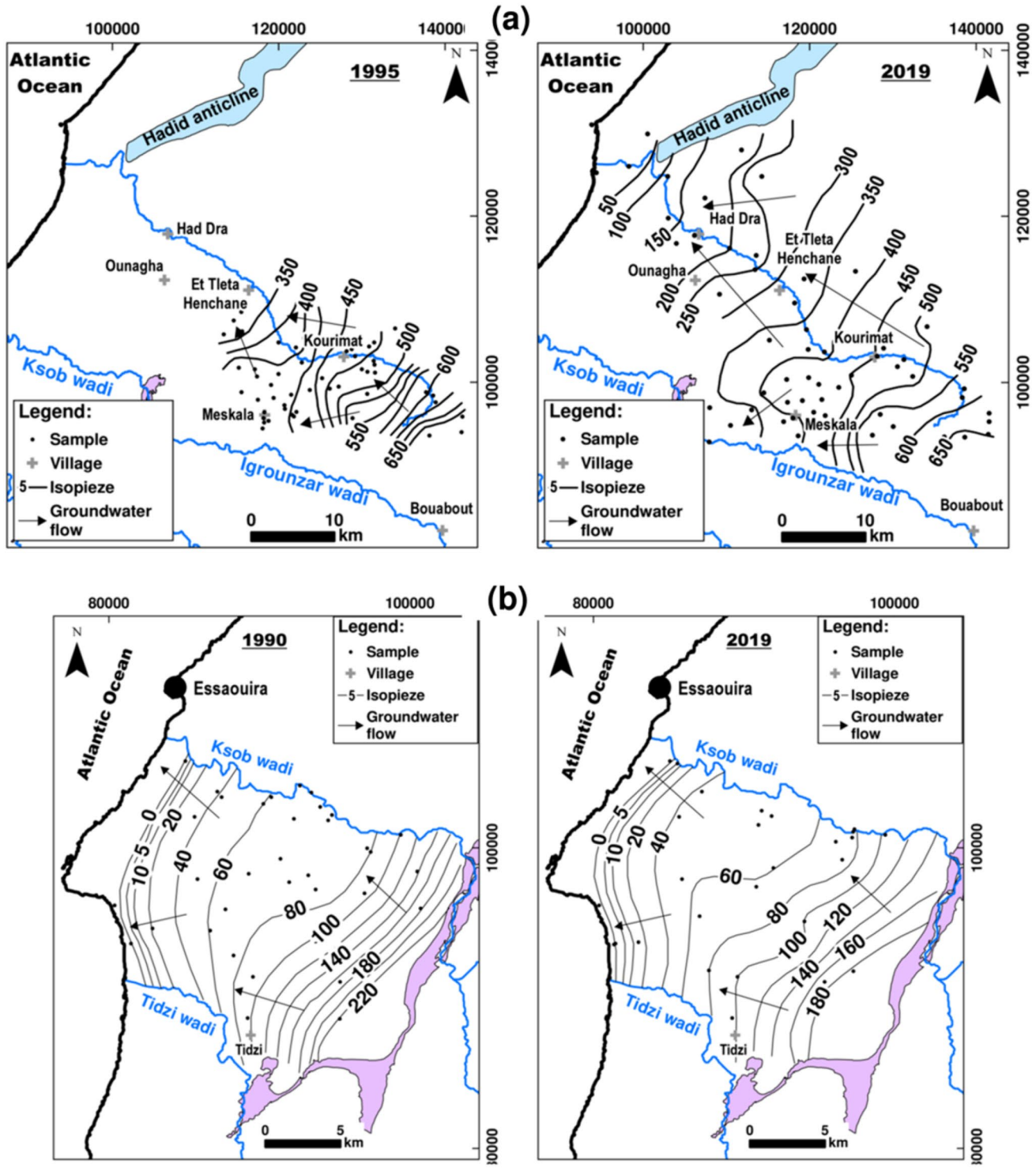

Fig. 5 Piezometric maps of the aquifer **a** Cenomanian–Turonian and **b** Plio-Quaternary

isopiezes 40 and 180 m more and more to the upstream, and this on the two piezometric maps. The piezometric level evolution of the wells capturing this aquifer and having experienced measurements of their water body during 1990, 1995, 2000, 2004, 2009, 2015, 2017, 2018, and 2019 (Table 2) shows a reduction in the water table at these wells. It reached 17 m at well 261/51 and 6.6 m at well 140/51, between 1990 and 2019. The drought of 1995, the driest year in Morocco during the twentieth century, led to a general decline in the water level.

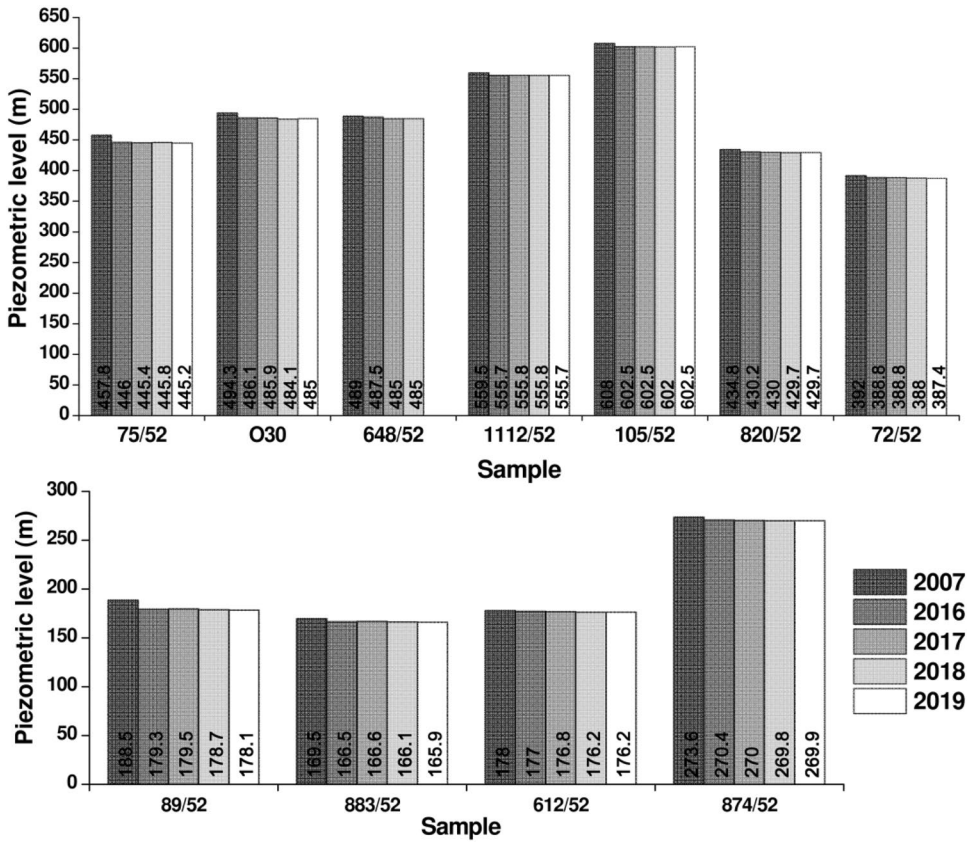

Fig. 6 Temporal evolution of the piezometric level of certain wells capturing the Cenomanian–Turonian aquifer

Table 2 Groundwater level evolution of some wells capturing the Plio-Quaternary aquifer

Well	PL1990	PL1995	PL2000	PL2004	PL2009	PL2015	PL2017	PL2018	PL2019	PL2019-PL1990
3/51	2.4	3.8	4.2	4.5	3.0	0.7	nm	nm	−2.9	−5.3
11/51	−1.0	−1.8	−0.5	0.0	nm	−0.9	−1.0	−1.1	−1.2	−0.17
15/51	60.2	47.6	49.0	60.0	58.0	53.0	57.4	56.9	56.8	−3.35
27/51	169.5	156.9	164.0	173.0	nm	171.8	170.3	nm	170.3	0.78
140/51	50.2	50.3	50.5	51.5	nm	43.6	43.8	43.5	43.6	−6.66
261/51	nm	89.9	86.2	87.5	nm	nm	72.3	nm	72.5	−17.45
272/51	76.4	79.3	81.1	69.5	nm	nm	76.4	76.9	76.0	−0.4

PL stands for piezometric level (in m); nm stands for not measured

According to Fekri [15], differential gauges carried out during the hydrological cycle 1990–1991 demonstrated a supply of the Plio-Quaternary aquifer from the wadi Ksob (perennial stream, which becomes intermittent in recent years) with a flow rate of 42 l/s. Also, this aquifer is also recharged by direct infiltration of precipitation with an estimated volume of 50.5 l/s [15].

According to the National Office for Drinking Water (ONEP), the total volume pumped by boreholes capturing the Plio-Quaternary aquifer is 39.5 l/s. The samples taken from traditional wells (0.05 l/s/well [15]) as well as a loss at the outputs (of the order of 54.7 l/s [15]) increase the output balance at 99.2 l/s.

The comparison of the "inputs and outputs balance" shows a slight difference of 6.7 l/s. The study by Bahir et al. [5] showed that the piezometric level within the Essaouira basin is closely related to precipitation; this is confirmed by Ouhamdouch et al. [29]. Given that the study sector is characterized by an absence of industrial activity, the agricultural activity practiced by the population is of the "subsistence type", and that the difference between the inputs and the outputs balance sheet is small, the effect of overexploitation and agricultural activity on the groundwater in the study area is negligible compared to the effect of climate change.

However, the decrease in the piezometric level could only be explained by the decrease in precipitation under the effect of climate change.

4.3 Hydrogeochemistry

Hydrogeochemical approach is a valuable tool to characterize groundwater chemistry. The latter is largely influenced by the characteristics of the host rock, by the hydrodynamics of the aquifers, and also by the climatic and exploitation conditions.

4.3.1 Chemical facies

To specify the chemical facies of groundwater in the study area, the major element composition has been plotted on the Piper diagram [32].

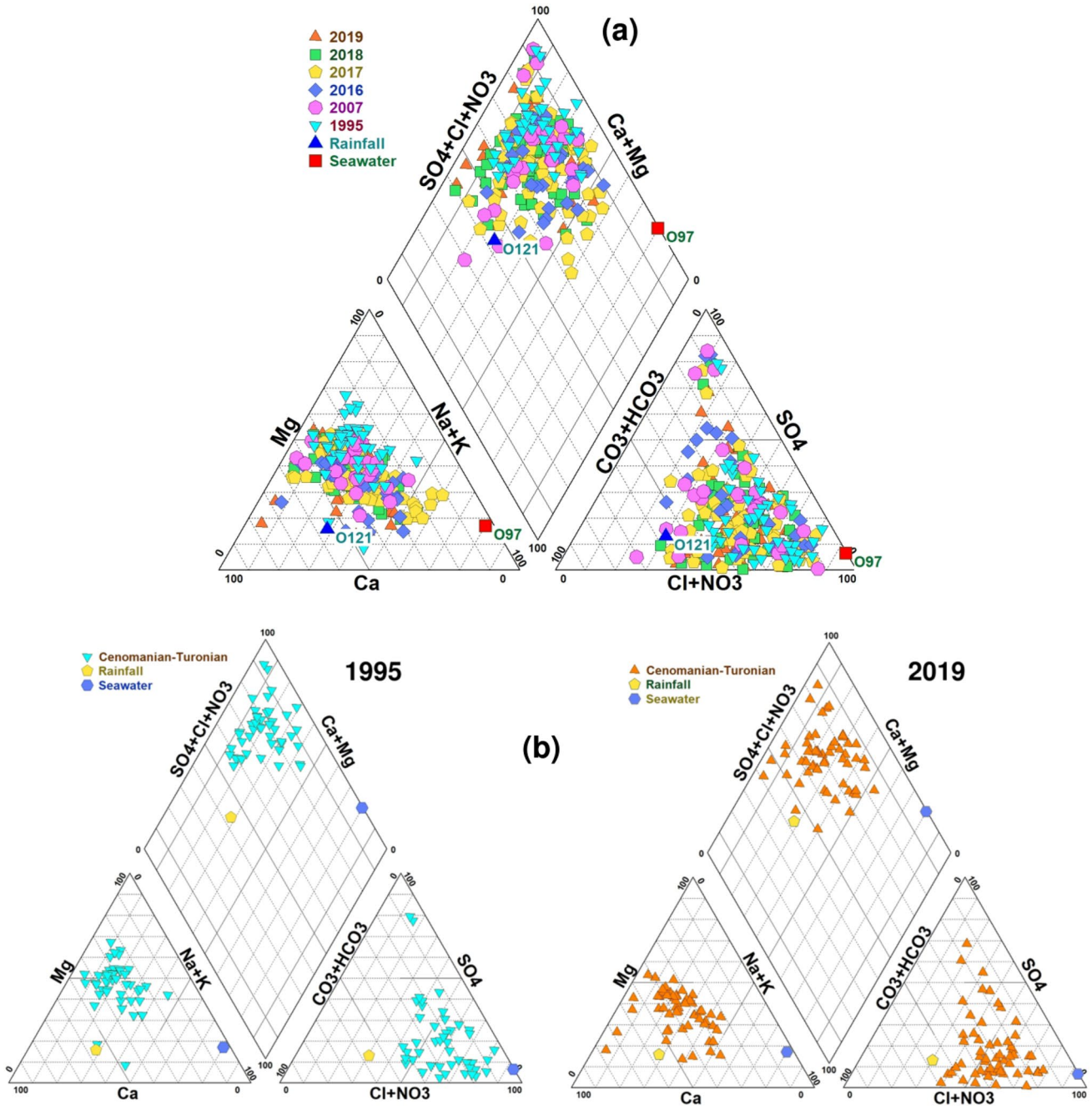

Fig. 7 Piper diagram of analysed samples of **a** Cenomanian–Turonian aquifer from 1995 to 2019 and **b** comparison between samples of 1995 and 2019

-For the Cenomanian–Turonian aquifer, representing the upstream part of the study basin, the projection of the analysed samples on the Piper diagram (Fig. 7a) shows that the waters have a mixed facies between Cl–Na, Cl–Ca–Mg, SO_4–Ca–Mg, and HCO_3–Ca–Mg. In 1995, the majority of the samples present a Cl–Ca–Mg facies. For the samples of the 2007 campaign, the chemical facies are of Cl–Ca–Mg, SO_4–Ca–Mg, and HCO_3–Ca–Mg type with the dominance of the Cl–Ca–Mg type. As for the samples analysed in 2016, they have a facies Cl–Na, Cl–Ca–Mg, and SO_4–Ca–Mg type. For the 2017, 2018, and 2019 campaigns, we note that the analysed waters present four types of facies: Cl–Na, Cl–Ca–Mg, SO_4–Ca–Mg, and HCO_3–Ca–Mg with the dominance of the Cl–Ca–Mg type. A comparison of the results of the 1995 campaign and those of 2019 (Fig. 7b) shows that the groundwater facies of the Cenomanian–Turonian aquifer have experienced a slight change.

-For the downstream part, the analysis of Piper diagrams for the Plio-Quaternary and Turonian aquifers (Fig. 8a and b) shows that they are classified under a mixed facies between Cl–Na and Cl–Ca–Mg. The grouping of points of the Plio-Quaternary aquifer close to those of the Turonian aquifer suggests an interconnection between these two aquifers.

The comparison between the results of 1990 and 2019 is presented in Fig. 8c. This shows that there is a slight

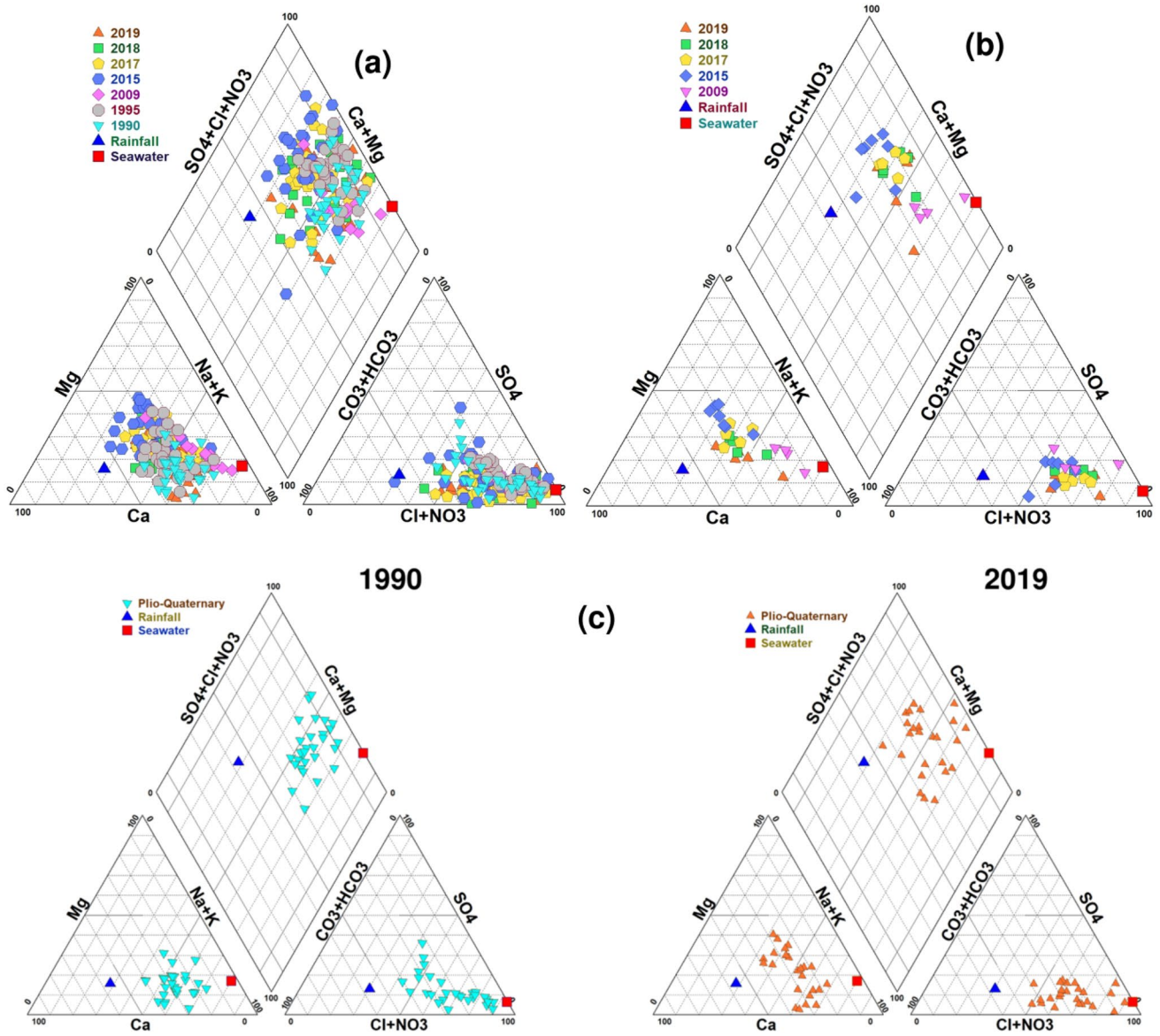

Fig. 8 Piper diagram of analysed samples of **a** Plio-Quaternary from 1990 to 2019 and of **b** Turonian from 2009 to 2019, and **c** comparison between samples of 1990 and 2019 for the Plio-Quaternary aquifer

evolution in the chemical facies of the Plio-Quaternary groundwater. Indeed, on the cations triangle concerning the 1990 campaign, the majority of the points have a percentage higher than 50% in Na with a tendency towards the Na pole. However, in 2019, the majority of the points do not exceed 50% in Na with a tendency towards the centre of the triangle "no dominant cations". For the anion triangle, a clear dominance of Cl is noted, whether in 1990 or in 2019. The position of some samples relative to the sample representing seawater on the Piper diagram suggests that the Plio-Quaternary aquifer is probably affected by the marine intrusion.

4.3.2 Groundwater mineralization

To determine the origin and the main processes responsible for the groundwater mineralization of the study area, the correlations between the main major elements have been studied.

Chloride is a conservative ion that is always found in natural waters at very variable contents [16], and sodium is generally associated with chlorides. Chloride concentrations in groundwater of the upstream part vary from 113 to 1818 mg/l with an average of 574 mg/l. As for those of sodium, they vary between 12 and 541 mg/l with an average of 167 mg/l. According to the Piper diagram (Fig. 7), the Cl ions are the most dominant in the groundwater. For the downstream part, the Cl contents vary between 227 and 4800 mg/l with an average of 809 mg/l and the Na concentrations vary between 84 and 1950 mg/l with an average of 351 mg/l.

The Na versus Cl correlation diagram (Fig. 9a) shows a significant positive correlation between these two ions. This reflects that these two elements have probably the same origin. Some points are scattered around the halite dissolution line (line 1:1), reflecting the contribution of this mineral in the groundwater mineralization. This hypothesis is confirmed by negative values of the saturation indices with respect to this mineral (Fig. 10). The rest of the samples are located below the line 1:1 and parallel to it, reflecting a Na deficit. This suggests the contribution of a phenomenon other than the halite dissolution in the groundwater mineralization.

The Na deficit compared to Cl could be linked to the bases exchange reactions, as shown in Fig. 9f, with the aquifer matrix, where the Na ions are fixed by the complex and replaced by Ca ions according to Eq. 1 [8]:

$$Na^{+} + \frac{1}{2}Ca - X_2 \rightarrow Na - X + \frac{1}{2}Ca^{2+} \quad (1)$$

with X being the aquifer matrix.

Also, an excess of Na could be explained by the second type of cations exchange where the Ca and/or Mg ions will be released in water and the Na ions will be fixed by the matrix according to Eq. 2:

$$\frac{1}{2}Ca^{2+} + Na - X \rightarrow \frac{1}{2}Ca - X_2 + Na^{+} \quad (2)$$

The Ca contents of the groundwater in the upstream part vary between 82 and 770 mg/l with an average of 214 mg/l. As for those of SO_4, they vary between 13 and 1942 mg/l with an average of 339 mg/l. As for the downstream part, the Ca concentrations oscillate between 64 and 850 mg/l with an average of 164 mg/l, and those of SO_4 vary between 30 and 830 with an average of 145 mg/l.

Figure 9b shows the existence of a significant correlation between the Ca and SO_4 ions. Indeed, the points whose Ca/SO_4 molar ratio is close to 1 reflect the same origin of these two ions which could be the gypsum and/or anhydrite dissolution. This is confirmed by negative values of the saturation indices with respect to gypsum and/or anhydrite (Fig. 10). However, the excess of Ca compared to SO_4 observed for the majority of the points could be linked to the phenomenon of reverse bases exchange. Also, the saturation indices calculated for these points with respect to carbonate minerals are close to zero, or greater for some samples, corroborating that the enrichment of Ca is mainly due to the bases exchange phenomenon (Fig. 9f).

The Ca versus Mg diagram (Fig. 9c) shows a positive correlation between these two ions, and this reflects that these two elements come from the same origin. The majority of the points are scattered around the dolomite dissolution line (line 1:1), thus suggesting the contribution of the dissolution of this mineral to the groundwater mineralization. Other points are located above the line 1:1, confirming the contribution of the bases exchange process in the groundwater mineralization of the aquifers studied.

The Ca versus HCO_3 correlation (Fig. 9d) shows that these two elements do not have a significant correlation and that the majority of the analysed samples show a Ca/HCO_3 molar ratio greater than 1. This excess of Ca compared to HCO_3 ions translates the existence of other sources of calcium which could be the phenomenon of ions exchange and that of dedolomitization (incongruent dissolution of dolomite) [23] accompanied by simultaneous precipitation of calcite.

4.4 Nitrates contamination

The main source of nitrate in water is the leaching of nitrogenous products in the soil following the decomposition of organic matter or synthetic and/or natural fertilizers. The nitrate content of unpolluted natural waters is

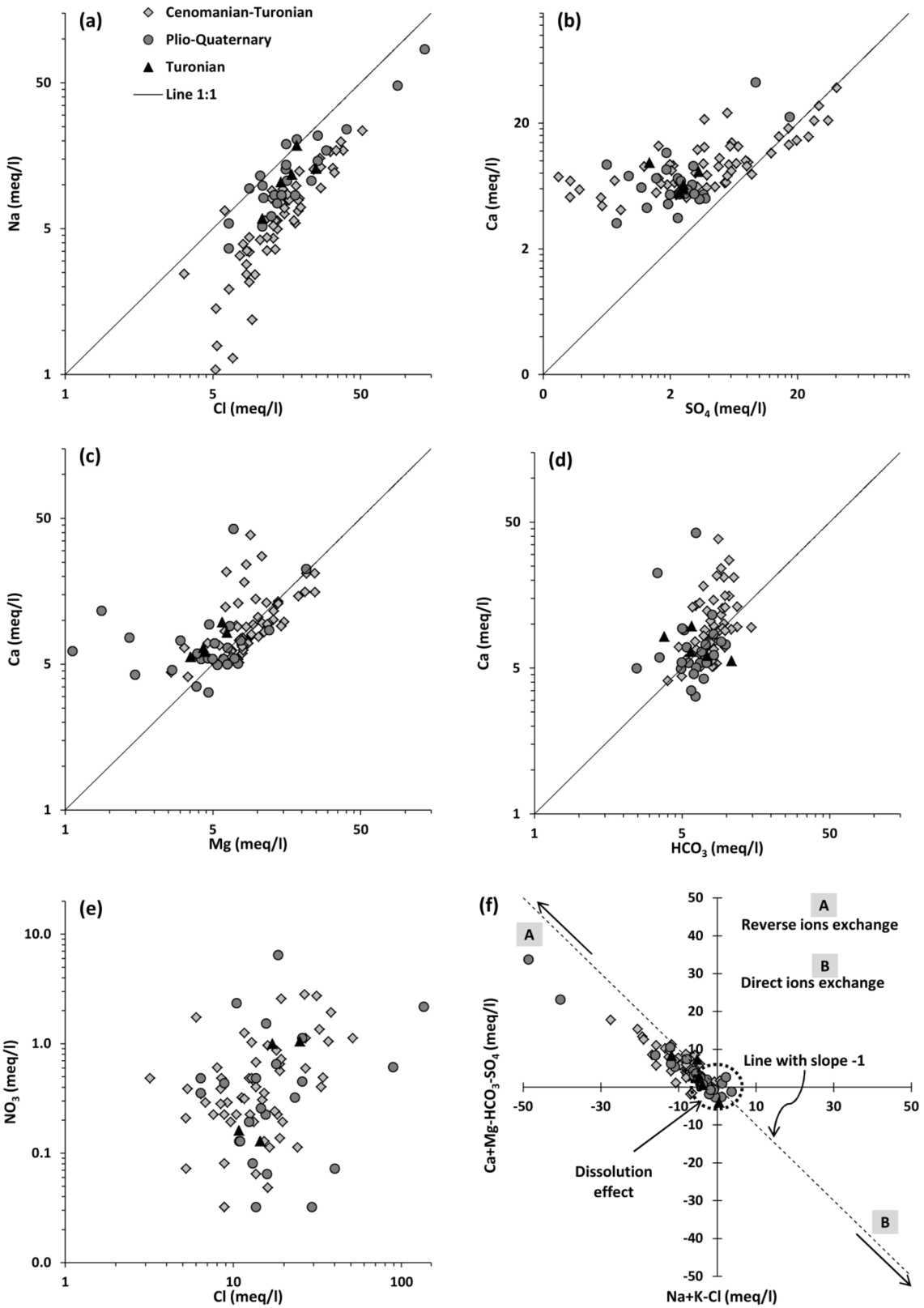

Fig. 9 Correlation diagram **a** Na versus Cl, **b** Ca versus SO_4, **c** Ca versus Mg, **d** Ca versus HCO_3, **e** NO_3 versus Cl, and **f** $(Ca + Mg - HCO_3 - SO_4)$ versus $(Na + K - Cl)$

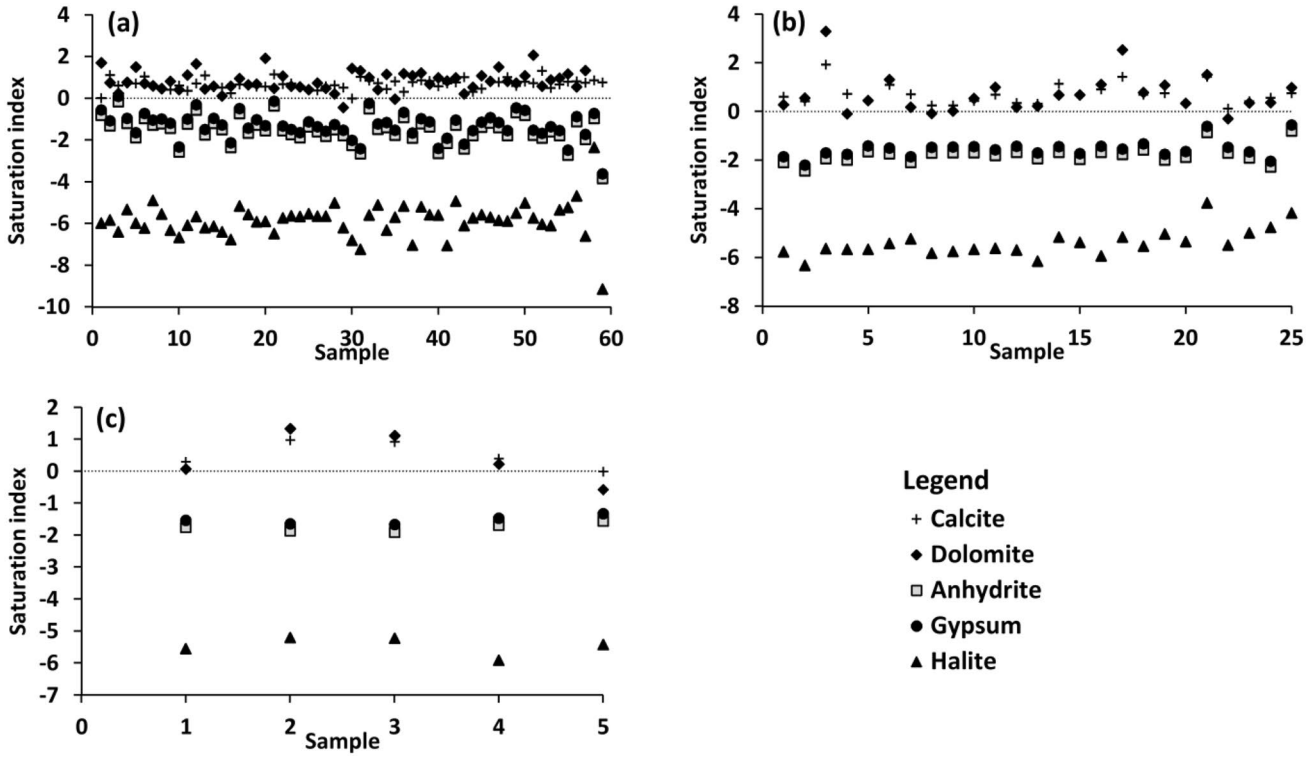

Fig. 10 Saturation indices of analysed samples of **a** Cenomanian–Turonian, **b** Plio-Quaternary and **c** Turonian

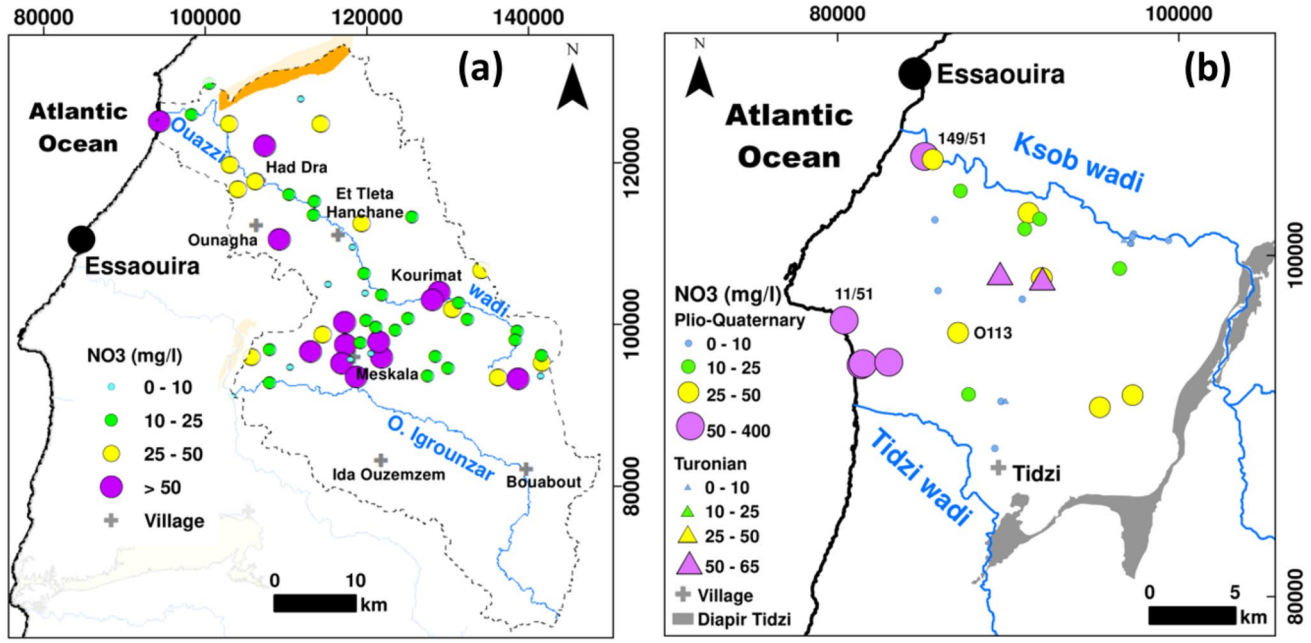

Fig. 11 Spatial distribution of NO_3 content in groundwater of **a** Cenomanian–Turonian and **b** Plio-Quaternary and Turonian

highly variable, varying from 1 to 15 mg/l depending on the season and the origin [10].

The NO_3 contents in groundwater of the Cenomanian–Turonian aquifer (upstream part) vary from 0 to 175 mg/l with a punctual spatial distribution (Fig. 11a).

Generally, levels are high in the Meskala region and exceed the threshold (50 mg/l) set by the World Health Organization [37]. Also, high values have been noted in some other wells such as 613/52, O37, 75/52, and O56. This could be explained by traditional methods of drawing which cause that a significant part of water flowing around the wells constitutes quasi-permanent puddles which enrich NO3 by livestock excrement during watering. For the Plio-Quaternary and Turonian aquifers, the NO_3 contents vary, respectively, between 0 and 400 mg/l and between 0 and 65 mg/l (Fig. 11b).

The very weak correlation between Cl and NO_3 (Fig. 9e) makes it possible to say that the levels of NO_3 assayed in the samples analysed are not of agricultural origin since the chlorides are due to the dissolution of the evaporate minerals.

The highest concentrations within the Plio-Quaternary aquifer are recorded in the southwest part, near Cap Sim (wells 11/51, O94, and O95) and in the north-west, the tourist area of the Diabate (well 149/51). These high levels could be explained by the intense concentration of septic tanks constructed by the guest houses in the tourist area of Sidi Kaouki because of the absence of a sanitation network. As for the Turonian aquifer, only two points for each aquifer have levels exceeding the limit set by WHO [37].

The contamination of the other wells could be explained by traditional methods of drawing which cause that a significant part of water flowing around the wells constitutes quasi-permanent puddles which enrich NO_3 by livestock excrement during watering.

4.5 Evolution of groundwater salinity

The groundwater salinization is a very marked phenomenon in areas of water scarcity, especially the Saharan, arid and semi-arid zones. The scarcity or even the absence of surface water and the increasing demand for water as well as the decrease in precipitation have created enormous pressures on groundwater which have thus resulted in the degradation of their quality.

The spatial–temporal distribution of salinity was studied to assess the impact of climate change on the groundwater quality of the study area. For the upstream part, the 1995 campaign shows the salinity values vary between 0.2 and 1.9 g/l with an average of 0.7 g/l. In 2007, the salinity values fluctuated between 0.5 and 2.4 g/l with an average of 1.1 g/l. As for the 2016 campaign, its values vary between 0.3 and 4.6 g/l with an average of 1.37 g/l. For the 2017 campaign, the salinity fluctuates between 0.3 and 4 g/l with an average of 1.29 g/l. In 2018, the salinity values vary between 0.4 and 4.3 g/l with an average of 1.4 g/l and between 0.35 and 4.4 g/l with an average of 1.4 for samples from the 2019 campaign (Fig. 12).

From the analysis of the maps in Fig. 12, it can be seen that the salinity values become more and more important by advancing in time and going from east to west, and this during the six campaigns. Taking, for example, the region of Sebt Kourimat, recharge area of the Cenomanian–Turonian aquifer, the salinity values fluctuate around 0.46 g/l in 1995 to reach 2.9 g/l in 2019. However, the general spatial–temporal evolution of salinity shows an increasing trend.

For the downstream part, the groundwater of the Plio-Quaternary aquifer has salinity values varying between 0.6 and 3.4 g/l with an average of 1.7 g/l in 1990, between 0.9 and 3 g/l with an average of 1.6 g/l in 1995, from 0.4 to 4.1 g/l with an average of 1.3 g/l in 2004, between 0.9 and 2.2 g/l with an average of 1.4 g/l in 2009, from 0.3 to 4.7 with an average of 1.5 g/l in 2015, between 0.4 and 4.8 g/l with an average of 1.53 g/l in 2017, between 0.5 and 6.5 g/l with an average of 1.6 g/l in 2018 and between 0.46 and 8.4 g/l with an average of 1.7 g/l in 2019 (Fig. 13). From the maps of Fig. 13, the highest values are observed in the southern and western part and this further to the remoteness to the recharge zones, to the residence time, to the influence of the Triassic terrains, and to the influence of the sea [marine intrusion (well 11/51)], while the low values are recorded in the northern part (along the Ksob wadi) and in the east which represent the recharge zones of the Plio-Quaternary aquifer. The temporal evolution of the groundwater salinity of the Plio-Quaternary aquifer shows an upward trend going from year to year and consequently deterioration in the groundwater quality. As for the Turonian aquifer, the minimum values of salinity are around 0.8 g/l and the maximum values are around 1.3 g/l with an average of 1.1 g/l, and this for 2004, 2009, 2015, 2017, 2018 and 2019 campaigns (Fig. 13). The temporal evolution of the groundwater salinity of this aquifer does not show a significant trend, and this could be explained by its significant depth and its captive nature.

As the study area is under a semi-arid climate, with a tendency towards an arid climate in recent years accompanied by a decrease in precipitation and an increase in the temperature, which frequently causes intense periods of drought resulting in evaporation that affects surface and groundwater, especially the shallow waters, the degradation of the groundwater quality is mainly due to this situation and the decrease in the piezometric level caused by climate change.

5 Conclusion

As the other basins from the coastal zones, the Essaouira basin has not been spared from the effect of climate change. The combination of hydroclimatic, piezometric,

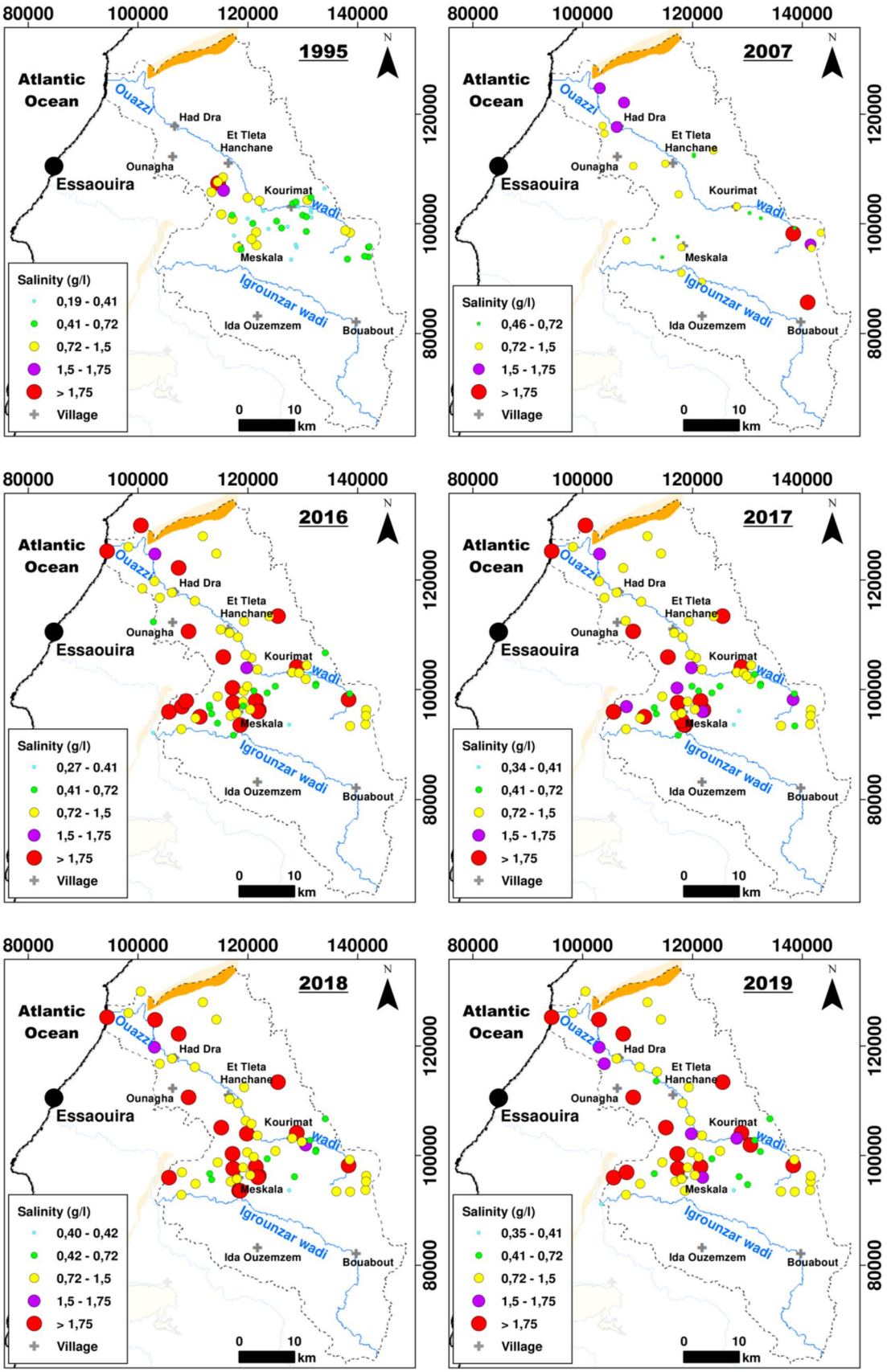

Fig. 12 Spatial distribution of salinity in Cenomanian–Turonian aquifer

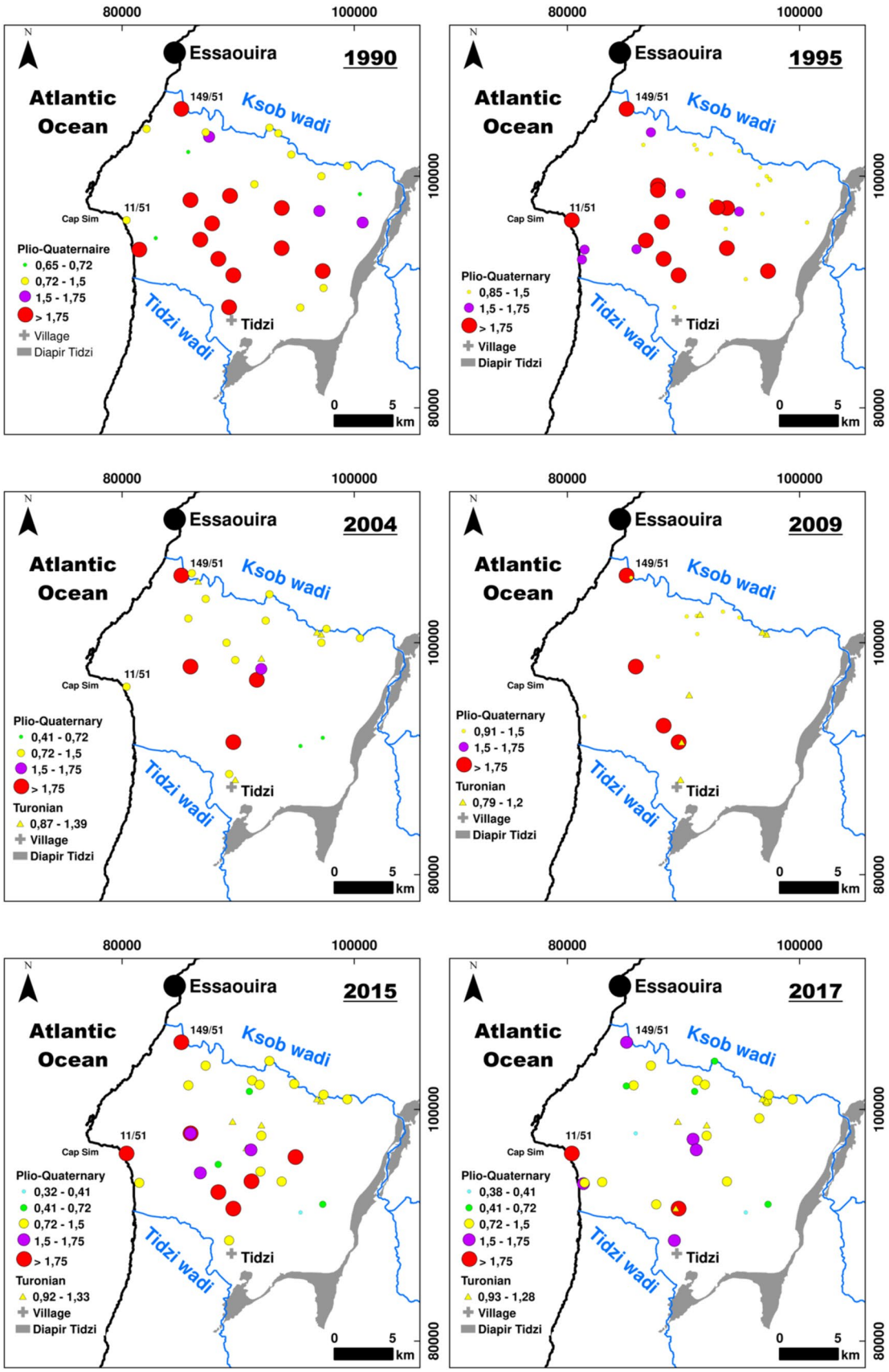

Fig. 13 Spatial distribution of salinity in Plio-Quaternary and Turonian aquifers

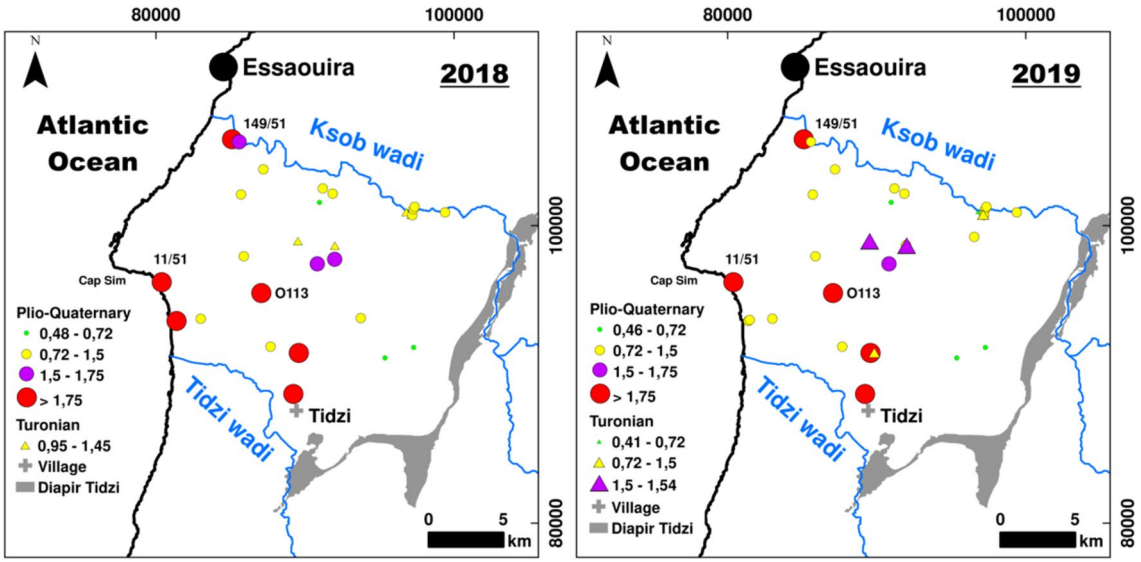

Fig. 13 (continued)

and hydrogeochemical approaches in the study of the groundwater resource within the Essaouira basin led to the following conclusions:

Analysis of precipitation evolution using the Pettitt and Mann–Kendall statistical tests made it to detect a downward trend in precipitation in the whole basin of the order of 12–16%. This decrease is accompanied by significant warming of the order of 1.2–2.3 °C. This will undoubtedly hurt the groundwater recharge.

The piezometric approach has shown that the Cenomanian–Turonian and Plio-Quaternary aquifers have retained the general flow direction of their groundwater, during the study period. Monitoring the piezometry over a period of 24 years (1995–2019) for the Cenomanian–Turonian aquifer and 29 years (1990–2019) for the Plio-Quaternary aquifer shows a continuous drop in the piezometric level which exceeds 12 m for the Cenomanian–Turonian aquifer, 17 m for the Plio-Quaternary aquifer.

The general downward trend in the piezometric level could be explained by the decrease in precipitation caused by climate change.

The results of hydrochemical approach show that the groundwater of the Cenomanian–Turonian aquifer presents the Cl–Ca–Mg, Cl–Ca, Cl–Na, and HCO_3–Ca mix facies with the dominance of the Cl–Ca–Mg mix and Cl–Ca facies. The study of the temporal evolution of these facies shows that there has been a slight change. The groundwater of the Plio-Quaternary and Turonian aquifers is of mixed type between Cl–Na and Cl–Ca–Mg. The chemical facies experienced a slight evolution from the Cl–Na facies to the Cl–Na and Cl–Ca–Mg facies for the Plio-Quaternary aquifer and from the Cl–Na facies to the Cl–Ca–Mg facies for the Turonian aquifer.

The correlations established between the major element concentrations show that the groundwater mineralization is controlled by the dissolution of evaporate (halite, gypsum, and/or anhydrites) and carbonates (dolomite) minerals, by the bases exchange phenomenon, and by the marine intrusion, especially at the Plio-Quaternary aquifer. The study of the spatio-temporal evolution of the groundwater quality shows a gradual deterioration in time and space.

As the study area is under a semi-arid climate, with a decrease in precipitation and an increase in the temperature, which frequently causes intense periods of drought resulting in evaporation that affects surface and groundwater, especially the shallow waters, the groundwater quality degradation is mainly due to this situation and to the decrease in the piezometric level caused by climate change.

However, the Essaouira basin is vulnerable to climate change because its recharge is entirely dependent on precipitations.

Compliance with ethical standards

Conflict of interest The authors declare that they have no conflict of interest.

Appendix

Results of physico-chemical analyses

Parameter	pH	T (°C)	EC (µs/cm)	Ca (meq/l)	Mg (meq/l)	Na (meq/l)	K (meq/l)	HCO_3 (meq/l)	Cl (meq/l)	SO_4 (meq/l)	NO_3 (meq/l)
Campaign 2019											
Cenomanian–Turonian aquifer											
	N = 57										
Minimum	7.0	14.9	615	4.1	2.6	0.5	0.0	4.0	3.2	0.3	0.0
Maximum	8.4	24.0	5738	38.4	24.5	23.5	4.3	14.7	51.3	40.4	2.8
Median	7.5	20.8	2203	9.0	8.3	6.3	0.2	8.0	13.6	3.9	0.4
Mean	7.5	20.5	2428	10.7	9.7	7.3	0.4	8.2	16.2	7.1	0.6
SD	0.3	1.8	1182	6.4	4.8	5.1	0.7	1.9	9.7	8.8	0.6
Plio-Quaternary aquifer											
	N = 29										
Minimum	7.1	17.3	880	3.2	0.6	3.7	0.0	2.5	6.4	0.6	0.0
Maximum	9.2	25.0	12,250	42.4	21.4	84.8	1.9	9.8	135.4	17.3	6.5
Median	7.6	21.4	2041	5.7	5.0	10.3	0.2	6.2	15.4	2.3	0.3
Mean	7.7	21.4	2855	8.2	5.6	15.6	0.3	6.2	23.6	3.1	0.7
SD	0.5	1.8	2564	7.9	4.1	16.7	0.5	1.8	27.9	3.3	1.3
Turonian aquifer											
	N = 5										
Minimum	7.1	20.0	1833	5.6	3.5	5.9	0.1	3.8	10.8	1.4	0.0
Maximum	7.8	26.5	2800	9.7	6.2	18.6	0.3	10.8	24.8	3.3	1.0
Median	7.3	24.8	2287	6.5	4.4	11.7	0.1	5.8	17.1	2.5	0.2
Mean	7.4	23.9	2310	7.2	4.8	11.9	0.2	6.7	17.1	2.4	0.5
SD	0.3	2.6	423	1.7	1.1	4.6	0.1	2.6	5.2	0.7	0.5
Campaign 2018											
Cenomanian–Turonian aquifer											
	N = 62										
Minimum	7.2	16.2	601	3.3	2.5	0.5	0.0	3.1	2.4	0.1	0.1
Maximum	9.6	24.6	6845	29.1	27.1	24.4	0.9	11.3	48.1	46.2	2.7
Median	7.8	20.9	2195	7.4	8.0	5.9	0.1	6.1	10.8	4.3	0.4
Mean	8.0	20.9	2482	8.8	9.5	6.6	0.1	6.3	14.0	5.9	0.6
SD	0.6	1.6	1309	4.9	5.3	4.5	0.2	1.5	10.0	7.4	0.6
Plio-Quaternary aquifer											
	N = 24										
Minimum	7.2	17.6	916	2.9	1.2	3.3	0.0	2.3	2.8	0.1	0.0
Maximum	8.4	26.3	9744	18.2	19.6	63.7	1.7	9.0	89.1	8.5	6.4
Median	7.6	22.0	2176	5.6	5.8	7.8	0.2	4.4	12.4	2.4	0.3
Mean	7.7	22.0	2850	7.2	5.9	12.9	0.3	4.6	19.5	2.5	0.7
SD	0.3	1.8	1987	4.4	3.6	13.4	0.4	1.5	19.1	2.0	1.4
Turonian aquifer											
	N = 6										
Minimum	6.0	21.5	48	0.1	0.2	0.0	0.1	0.2	0.1	0.0	0.0
Maximum	7.9	27.1	2699	7.9	6.9	12.0	0.4	6.3	16.3	3.8	1.0
Median	7.3	23.5	2241	5.9	5.5	8.7	0.1	4.4	13.5	3.0	0.2
Mean	7.3	24.1	1972	5.3	4.8	7.9	0.2	4.1	11.4	2.6	0.4
SD	0.7	2.3	989	2.8	2.4	4.3	0.1	2.1	6.0	1.3	0.4
Campaign 2017											
Cenomanian–Turonian aquifer											
	N = 67										
Minimum	6.9	17.9	635	0.0	0.0	0.0	0.0	0.0	0.0	0.0	0.0
Maximum	8.1	29.3	6776	26.7	25.2	33.1	2.1	11.2	69.7	30.0	3.1
Median	7.4	21.3	1936	7.3	7.8	5.4	0.1	6.3	10.8	3.6	0.5
Mean	7.4	21.4	2318	8.3	8.7	8.1	0.1	6.3	15.0	5.5	0.7
SD	0.3	1.8	1234	5.1	5.1	6.9	0.3	1.9	13.1	6.0	0.7

Parameter	pH	T (°C)	EC (µs/cm)	Ca (meq/l)	Mg (meq/l)	Na (meq/l)	K (meq/l)	HCO_3 (meq/l)	Cl (meq/l)	SO_4 (meq/l)	NO_3 (meq/l)
Plio-Quaternary aquifer											
	N = 27										
Minimum	7.1	18.9	724	2.2	2.6	3.7	0.1	3.1	4.8	0.2	0.1
Maximum	8.0	25.4	7555	18.4	16.9	62.2	1.9	9.3	88.5	5.4	2.0
Median	7.6	22.2	1859	5.7	6.2	8.1	0.3	5.2	14.4	1.8	0.3
Mean	7.6	22.1	2203	6.7	6.6	11.4	0.4	5.5	19.2	1.9	0.6
SD	0.2	1.6	1349	3.8	3.3	11.0	0.4	1.4	16.4	1.1	0.5
Turonian aquifer											
	N = 5										
Minimum	7.2	23.9	1892	4.8	5.8	6.6	0.2	4.7	13.2	2.0	0.1
Maximum	7.8	27.4	2442	8.7	7.7	10.4	0.5	6.2	19.2	3.4	0.6
Median	7.5	25.4	2293	6.0	6.6	9.3	0.2	6.0	16.0	2.7	0.2
Mean	7.5	25.4	2164	6.4	6.7	8.7	0.3	5.7	16.1	2.7	0.3
SD	0.2	1.5	254	1.5	0.7	1.8	0.1	0.6	2.7	0.5	0.2
Campaign 2016											
Cenomanian–Turonian aquifer											
	N = 74										
Minimum	6.9	16.4	493	3.8	1.1	1.6	0.0	3.6	2.2	0.4	0.0
Maximum	8.2	24.3	7600	28.5	22.2	22.2	2.6	7.7	29.3	46.2	6.3
Median	7.4	20.9	2000	7.4	6.9	5.2	0.1	4.9	8.0	5.0	1.0
Mean	7.4	21.0	2384	9.4	7.8	7.3	0.2	5.1	10.5	7.7	1.2
SD	0.2	1.6	1418	5.9	4.1	5.4	0.5	1.1	8.3	9.6	1.2
Campaign 2015											
Plio-Quaternary aquifer											
	N = 27										
Minimum	7.5	20.6	626	2.2	1.1	1.2	0.3	0.2	1.3	0.1	0.0
Maximum	8.2	25.0	7840	19.5	18.1	20.1	5.8	9.2	54.0	9.7	3.8
Median	7.8	22.3	2210	6.0	7.0	4.8	2.5	4.6	9.6	2.6	0.5
Mean	7.8	22.5	2637	6.9	7.1	5.8	2.6	4.7	14.1	2.8	0.9
SD	0.2	1.3	1497	4.1	4.1	3.9	1.4	2.2	11.3	2.0	1.1
Turonian aquifer											
	N = 7										
Minimum	7.4	23.6	1920	4.0	5.7	3.1	1.4	4.2	8.6	1.6	0.0
Maximum	7.9	27.8	4190	10.0	11.3	5.7	5.3	16.8	18.3	3.9	1.2
Median	7.5	24.8	2260	6.0	8.1	4.2	2.7	5.2	10.2	3.3	0.3
Mean	7.6	25.7	2483	6.4	8.1	4.4	2.6	6.5	11.5	2.9	0.5
SD	0.2	1.8	797	1.9	1.7	1.1	1.4	4.5	3.4	0.9	0.5
Campaign 2009											
Plio-Quaternary aquifer											
	N = 14										
Minimum	6.7	15.5	770	1.5	2.0	1.6	0.1	1.1	2.1	0.6	0.0
Maximum	7.5	23.0	3780	2.3	3.8	19.1	0.3	3.6	21.6	2.7	3.2
Median	7.3	20.0	2215	2.0	3.2	9.3	0.1	2.9	9.8	2.3	0.5
Mean	7.3	20.1	2382	2.0	3.0	9.0	0.2	2.7	10.0	2.1	0.8
SD	0.2	1.8	833	0.2	0.5	4.5	0.1	0.7	5.0	0.7	0.9
Turonian aquifer											
	N = 6										
Minimum	7.1	21.0	1450	1.7	2.5	6.5	0.1	0.5	7.5	2.2	0.0
Maximum	7.7	27.0	2340	1.9	3.1	12.5	0.6	3.6	11.9	3.7	0.1
Median	7.3	23.8	1929	1.8	2.9	7.6	0.3	3.1	8.3	2.6	0.1
Mean	7.4	23.9	1911	1.8	2.8	8.6	0.3	2.6	9.0	2.7	0.1
SD	0.2	2.0	320	0.1	0.2	2.7	0.3	1.4	2.0	0.7	0.1

Parameter	pH	T (°C)	EC (µs/cm)	Ca (meq/l)	Mg (meq/l)	Na (meq/l)	K (meq/l)	HCO_3 (meq/l)	Cl (meq/l)	SO_4 (meq/l)	NO_3 (meq/l)
Campaign 2007											
Cenomanian–Turonian aquifer											
	N = 27										
Minimum	6.7	17.4	900	0.0	0.0	0.0	0.0	0.0	0.0	0.0	0.0
Maximum	7.8	29.5	3880	34.0	27.8	13.4	1.7	7.5	33.9	49.9	3.5
Median	7.2	22.8	1810	7.2	8.5	4.7	0.1	5.5	6.9	4.5	0.6
Mean	7.2	23.0	2000	9.0	9.7	5.3	0.2	5.0	9.7	8.6	0.6
SD	0.3	2.8	864	7.9	6.8	3.6	0.3	2.2	8.1	13.1	0.7
Campaign 1995											
Cenomanian–Turonian aquifer											
	N = 45										
Minimum	–	15.00	352	0.13	0.10	0.07	0.00	0.05	0.08	0.01	0.00
Maximum	–	23.00	3060	1.41	1.90	1.00	0.01	0.14	1.40	1.00	0.08
Median	–	19.00	1020	0.35	0.54	0.22	0.00	0.10	0.21	0.08	0.01
Mean	–	19.13	1214	0.44	0.66	0.30	0.00	0.10	0.32	0.15	0.02
SD	–	1.61	697	0.30	0.42	0.25	0.00	0.02	0.27	0.21	0.02
Plio-Quaternary aquifer											
	N = 34										
Minimum	–	15.5	1590	4.6	1.6	7.2	0.0	1.7	11.9	0.9	0.0
Maximum	–	24.5	5040	18.8	12.3	32.0	0.9	6.8	48.8	8.7	4.4
Median	–	21.0	2595	8.1	6.1	14.3	0.1	4.7	21.4	3.4	1.2
Mean	–	21.1	2876	9.2	6.6	15.9	0.1	4.6	25.1	3.8	1.5
SD	–	1.8	921	4.1	2.4	6.8	0.1	1.2	11.7	1.6	1.2
Campaign 1990											
Plio-Quaternary aquifer											
	N = 29										
Minimum	7.7	15.0	1197	2.8	0.6	7.5	0.1	6.1	3.0	0.6	–
Maximum	8.6	25.0	5654	17.0	16.4	35.0	0.5	44.0	7.7	6.6	–
Median	8.1	21.0	2993	7.2	4.0	15.0	0.1	16.8	5.1	2.8	–
Mean	8.1	20.7	2881	8.4	4.8	17.1	0.2	19.3	4.9	3.0	–
SD	0.2	2.0	1392	3.9	3.3	8.2	0.1	11.3	1.3	1.3	–

References

1. Alpert P, Krichak SO, Shafir H, Haim D, Osetinsky I (2008) Climatic trends to extremes employing regional modeling and statistical interpretation over the E. Mediterranean. Glob Planet Change 63:163–170
2. Amghar M (1989) Apports des méthodes d'analyses de la tectonique cassante à la connaissance de l'histoire alpine du Haute Atlas Occidental. L'exemple du versant nord du bloc ancien et de l'Atlas d'Agadir (Haut Atlas, Maroc). Thèse 3ème cycle, Université Cadi Ayyad, Maroc
3. Babqiqi A (2014) Changements climatiques au Maroc: Étude du cas de la région de Marrakech Tensift Al Haouz et implications sur l'agriculture à l'horizon 2030. Thèse de doctorat, Université Cadi Ayyad, Maroc, 143 p
4. Bahir M, Mennani A, Jalal M, Fakir Y (2002) Impact de la sécheresse sur les potentialités hydriques de la nappe alimentant en eau potable la ville d'Essaouira (Mogador, Maroc). Sécheresse 13:13–19
5. Bahir M, Ouhamdouch S, Carreira PM (2016) La ressource en eau au Maroc face aux changements climatiques; cas de la nappe Plio-Quaternaire du bassin synclinale d'Essaouira. Comun Geol 103:35–44
6. Bahir M, Ouhamdouch S, Carreira PM, Chkir N, Zouari K (2018) Geochemical and isotopic investigation of the aquifer system under semi-arid climate: case of Essaouira basin (Southwestern Morocco). Carbonates Evaporites 33:65–77
7. Bahir M, Ouazar D, Ouhamdouch S (2019) Hydrogeochemical investigation and groundwater quality in Essaouira region, Morocco. Mar Freshwater Res 70:1317–1332
8. Capaccioni B, Didero M, Paletta C, Didero L (2005) Saline intrusion and refreshening in a multilayer coastal aquifer in the Catania Plain (Sicily, Southern Italy): dynamics of degradation processes according to hydrochemical characteristics of groundwaters. J Hydrol 307:1–16
9. Carreira PM, Bahir M, Ouhamdouch S, Fernandes PG, Nunes D (2018) Tracing salinization processes in coastal aquifers using an isotopic and geochemical approach: comparative studies in western Morocco and southwest Portugal. Hydrogeol J 26:2595–2615
10. Chenaker H, Houha B, Valles V (2017) Isotope studies and chemical investigations of hot springs from North-Eastern Algeria. J Mater Environ Sci 8:4253–4263
11. Dresh J (1962) Le Haut Atlas Occidental. Dans "Aspect de la géomorphologie du Maroc". Notes et Mémoire du Service Géologique-Maroc 96:107–121
12. Driouech F (2010) Distribution des précipitations hivernales sur le Maroc dans le cadre d'un changement climatique: descente

d'échelle et incertitudes. Thèse de doctorat, Université. Toulouse, France
13. Duffaud F (1960) Contribution à l'étude stratigraphique du bassin secondaire du Haut Atlas Occidental (Sud-Ouest du Maroc). Bull Soc Géol Fr 7:728–734
14. El Kharraz J, El-Sadekb A, Ghaffourc N, Mino E (2012) Water scarcity and drought in WANA countries. Procedia Eng 33:14–29
15. Fekri A (1993) Contribution à l'étude hydrogéologique et hydrogéochimique de la zone synclinale d'Essaouira (Bassin syncinal d'Essaouira). Ph.D. Thesis, Cadi Ayyad University, Marrakech, Morocco
16. Fetter CW (1993) Contaminant hydrogeology. Macmillan Publishing Company, New York, p 380
17. GIEC (2007) Résumé à l'intention des décideurs. In: Bilan 2007 des changements climatiques: Les bases scientifiques physiques. In: Solomon S, Qin D, Manning M, Chen Z, Marquis M, Averyt KB, Tignor M, Miller HL (eds) Contribution du Groupe de travail I au quatrième Rapport d'évaluation du Groupe d'experts intergouvernemental sur l'évolution du climat. Cambridge University Press, Cambridge
18. GIEC (2013) Climate Change 2013: the physical science basis. In: Stocker TF, Qin D, Plattner GK, Tignor M, Allen SK, Boschung J, Nauels A, Xia Y, Bex V, Midgley PM (eds) Contribution of Working Group I to the fifth assessment report of the intergovernmental panel on climate change. Cambridge University Press, Cambridge
19. Green TR, Makoto T, Henk K, Gurdak JJ, Allen DM, Hiscock KM, Holger T, Alice A (2011) Beneath the surface of global change: impacts of climate change on groundwater. J Hydrol 405:532–560
20. Jalal M, Blavoux B, Bahir M, Bellion Y, Laftouhi N, Puig JM, Mennani A, Daniel M (2001) Etude du fonctionnement du système aquifère karstique cénomano-turonien de l'oued Igrounzar (Bassin d'Essaouira, Maroc). J Afr Earth Sci 32(4):803–817
21. Kendall MG (1975) Multivariate nonparametric tests for trend in water quality. Water Resour Bull 24:505–512
22. Mann HB (1945) Nonparametric tests against trend. Econometrical 13:245–259
23. Marfia AM, Krishnamurthy RV, Atekwana EA, Panton WF (2004) Isotopic and geochemical evolution of ground and surface waters in a karst dominated geological setting: a case study from Belize, Central America. Appl Geochem 19:937–946
24. Mennani A (2001) Apport de l'hydrochimie et de l'isotopie à la connaissance du fonctionnement des aquifères de la zone côtière d'Essaouira (Maroc Occidental). Université Cadi Ayyad, Maroc, Thèse de doctorat, p 152p
25. Misra AK (2014) Climate change and challenges of water and food security. Int J Sustain Built Environ 3:153–165
26. Ouhamdouch S, Bahir M, Souhel A, Carreira PM (2016) Vulnerability and impact of climate change processes on water resource in semi-arid areas: in Essaouira Basin (Morocco). In: Grammelis P (ed) Energy, transportation and global warming, green energy and technology. Springer, Berlin, pp 719–736. https://doi.org/10.1007/978-3-319-30127-3_53
27. Ouhamdouch S, Bahir M (2017) Climate change impact on future rainfall and temperature in semi-arid areas (Essaouira Basin, Morocco). Environ Process 4:975–990
28. Ouhamdouch S, Bahir M, Carreira P (2018) Impact du changement climatique sur la ressource en eau en milieu semi-aride: exemple du bassin d'Essaouira (Maroc). RSE 31:13–27
29. Ouhamdouch S, Bahir M, Ouazar D, Carreira PM, Zouari K (2019) Evaluation of climate change impact on groundwater from semi-arid environment (Essaouira Basin, Morocco) using integrated approaches. Environ Earth Sci 78:449. https://doi.org/10.1007/s12665-019-8470-2
30. Ouhamdouch S, Bahir M, Ouazar D, Goumih A, Zouari K (2020) Assessment the climate change impact on the future evapotranspiration and flows from a semi-arid environment. Arab J Geosci 13:82. https://doi.org/10.1007/s12517-020-5065-x
31. Pettitt AN (1979) A non-parametric approach to the change-point problem. Appl Stat 28:126–135
32. Piper AM (1944) A graphic procedure in the geochemical interpretation of water analyses. Trans Am Geophys Union 25:914–923
33. Ragab R, Prudhomme C (2002) Climate change and water resources management in arid and semi-arid regions: prospective and challenges for the 21st century. Biosyst Eng 81:3–34
34. Rodier J, Legube B, Merlet N, et coll (2009) L'Analyse de l'eau. 9e édition, Dunod, ISBN 978-2-10-054179-9
35. Sebbar A, Badri W, Fougrach H, Hsaine M, Saloui A (2011) Etude de la variabilité du régime pluviométrique au Maroc septentrional (1935–2004). Sécheresse 22:139–148
36. Stour L, Agoumi A (2008) Sécheresse climatique au Maroc durant les dernières décennies. Hydroécol Appl 16:215–232
37. WHO (2011) Guidelines for drinking water quality, 4th edn. ISBN: 978 924 154815 1